

AD-A037 426

BALLISTIC RESEARCH LABS ABERDEEN PROVING GROUND MD
STRESSES PRODUCED IN A LONG CYLINDER BY A NUCLEAR THERMAL ENVIR--ETC(U)
FEB 77 E F QUIGLEY
BRL-1962

F/G 18/3

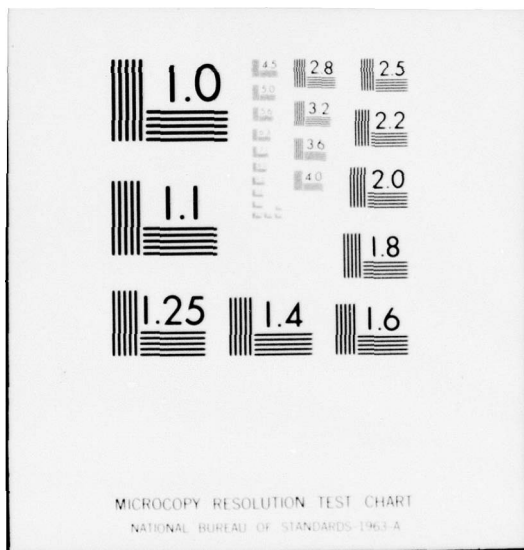
UNCLASSIFIED

NL

1 of 1
ADA037426



						END DATE FILMED 4-77							



MICROCOPY RESOLUTION TEST CHART
NATIONAL BUREAU OF STANDARDS-1963-A

BRL R 1962

BRL

12
B.S.

AD

ADA 037426

REPORT NO. 1962

STRESSES PRODUCED IN A LONG CYLINDER
BY A NUCLEAR THERMAL ENVIRONMENT

Ennis F. Quigley

February 1977

DDC
MAR 28 1977
RECEIVED

Approved for public release; distribution unlimited.

AD 1962

DDC FILE COPY

USA BALLISTIC RESEARCH LABORATORY
ABERDEEN PROVING GROUND, MARYLAND

Destroy this report when it is no longer needed.
Do not return it to the originator.

Secondary distribution of this report by originating
or sponsoring activity is prohibited.

Additional copies of this report may be obtained
from the National Technical Information Service,
U.S. Department of Commerce, Springfield, Virginia
22151.

The findings in this report are not to be construed as
an official Department of the Army position, unless
so designated by other authorized documents.

UNCLASSIFIED

SECURITY CLASSIFICATION OF THIS PAGE (When Data Entered)

REPORT DOCUMENTATION PAGE		READ INSTRUCTIONS BEFORE COMPLETING FORM
1. REPORT NUMBER BRL Report No. 1962 ✓	2. GOVT ACCESSION NO.	3. RECIPIENT'S CATALOG NUMBER
4. TITLE (and Subtitle) Stresses Produced in a Long Cylinder by a Nuclear Thermal Environment		5. TYPE OF REPORT & PERIOD COVERED FINAL repty
		6. PERFORMING ORG. REPORT NUMBER
7. AUTHOR(s) Ennis F./Quigley		8. CONTRACT OR GRANT NUMBER(s)
9. PERFORMING ORGANIZATION NAME AND ADDRESS USA Ballistic Research Laboratory Aberdeen Proving Ground, MD 21005		10. PROGRAM ELEMENT, PROJECT, TASK AREA & WORK UNIT NUMBERS 1W162118AH75
11. CONTROLLING OFFICE NAME AND ADDRESS US Army Materiel Development and Readiness Command 5001 Eisenhower Avenue Alexandria, VA 22333		12. REPORT DATE February 1977
		13. NUMBER OF PAGES 33
14. MONITORING AGENCY NAME & ADDRESS (if different from Controlling Office) 30p.		15. SECURITY CLASS. (of this report) UNCLASSIFIED
		15a. DECLASSIFICATION/DOWNGRADING SCHEDULE
16. DISTRIBUTION STATEMENT (of this Report) Approved for public release, distribution unlimited.		
17. DISTRIBUTION STATEMENT (of the abstract entered in Block 20, if different from Report)		
18. SUPPLEMENTARY NOTES		
19. KEY WORDS (Continue on reverse side if necessary and identify by block number) Nuclear Thermal Environment Thermal Stresses Plane Strain Solid Cylinder		
20. ABSTRACT (Continue on reverse side if necessary and identify by block number) (DTSebold) This report contains the plane strain derivation of a set of non-dimensional equations for the quasi-static, thermal stress field in a long, unrestrained, isotropic, homogeneous, solid cylinder whose lateral surface is subjected to heating by a nuclear thermal pulse. Included are the results of a parametric analysis of the stress field as a function of the rise time of the thermal pulse and the total energy of the pulse.		

DD FORM 1 JAN 73 1473

EDITION OF 1 NOV 65 IS OBSOLETE

UNCLASSIFIED

SECURITY CLASSIFICATION OF THIS PAGE (When Data Entered)

050 750

4B

	Page
I. INTRODUCTION.	5
II. TEMPERATURE EQUATION.	5
III. STRESS EQUATIONS.	8
IV. PARAMETRIC ANALYSIS	14
V. CONCLUSION.	29
GLOSSARY OF TERMS	30
DISTRIBUTION LIST	33

✓

ACCESSION for

White Section

Buff Section

NTS

DOC

UNANNOUNCED

JUSTIFICATION

LIST BY _____

DISTRIBUTION AVAILABILITY CODES

Dist. _____

A, AIR, and/or SPECIAL

A

PRECEDING PAGE BLANK - NOT FILMED

I. INTRODUCTION

When the lateral surface of a long, unrestrained, solid cylinder is exposed to a nuclear thermal radiation environment such as that indicated by Figure 1, both a transient, two dimensional, non axisymmetric temperature field¹ and a transient, three dimensional, thermal stress field are produced within the cylinder. Knowledge of the magnitude and type of these stresses is essential not only for thermal response analysis but also for the subsequent blast response analysis. This report describes a derivation of a set of non-dimensional equations for the stress field. Such equations will provide a convenient means for calculating the values of these stresses and for performing a parametric study of the equation variables. The results of such a parametric study involving t_0 and Q , two of the three nuclear pulse parameters, are also presented in this report.

The stress equations are derived within the framework of classical linear thermoelasticity theory using the plane strain assumption, and the approach is quasi-static in which inertia effects and thermoelastic coupling are neglected. Although the use of the plane strain assumption does not result in a solution valid for all the regions of the cylinder, it does provide a solution valid in the regions away from the ends of the cylinder.

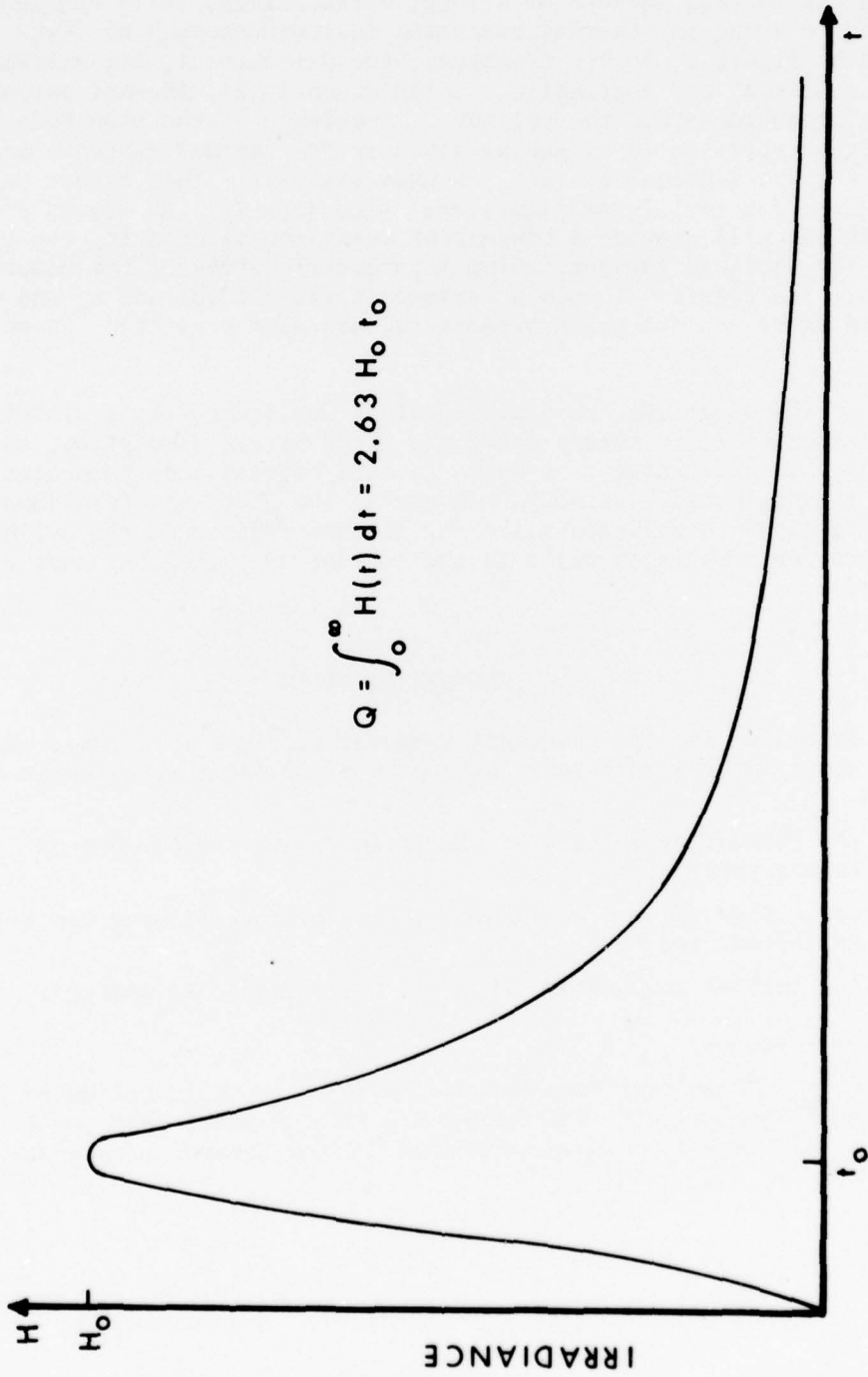
II. TEMPERATURE EQUATION

The equation² for the transient temperature field in a long, solid cylinder whose lateral surface is heated by a nuclear thermal environment for which

1. the thermal properties of the cylinder are independent of temperature,
2. convection and radiation heat losses by the cylinder can be neglected, and
3. the initial temperature field in the cylinder is uniform.

¹ E.F. Quigley, "Transient Temperatures Produced in Solid Cylinders by a Nuclear Thermal Pulse", BRL Report No. 1937, August, 1976, US Army Ballistic Research Laboratory, Aberdeen Proving Ground, Maryland.
(AD #A030703)

² *Ibid.*



$$Q = \int_0^{\infty} H(t) dt = 2.63 H_0 t_0$$

Figure 1. Nuclear Thermal Pulse

$$\begin{aligned}
\text{is: } T(r, \theta, t) = T_0 + \frac{2H_0}{\pi \rho c r_0} & \left\{ \int_0^t f(t) dt + \sum_{n=1}^{\infty} e^{-\lambda_{on}^2 \frac{\kappa}{\rho c} t} \left[\int_0^t e^{\lambda_{on}^2 \frac{\kappa}{\rho c} t'} \right. \right. \\
& \times \left. \left. \int_0^t f(t') dt' \right] J_0(\lambda_{on} r) + \frac{\pi}{2} \sum_{n=1}^{\infty} \frac{[\lambda_{1n} r_0]^2 e^{-\lambda_{1n}^2 \frac{\kappa}{\rho c} t}}{([\lambda_{1n} r_0]^2 - 1) J_1(\lambda_{1n} r_0)} \right. \\
& \times \left. \left[\int_0^t e^{\lambda_{1n}^2 \frac{\kappa}{\rho c} t'} f(t') dt' \right] J_1(\lambda_{1n} r) \cos \theta \right. \\
& - 2 \sum_{m=2}^{\infty} \sum_{n=1}^{\infty} \frac{[\lambda_{mn} r_0]^2 \cos(\frac{m\pi}{2}) e^{-\lambda_{mn}^2 \frac{\kappa}{\rho c} t}}{[m^2 - 1] [\lambda_{mn} r_0]^2 - m^2} J_m(\lambda_{mn} r_0) \\
& \times \left. \left[\int_0^t e^{\lambda_{mn}^2 \frac{\kappa}{\rho c} t'} f(t') dt' \right] J_m(\lambda_{mn} r) \cos m\theta \right. \quad (1)
\end{aligned}$$

where $H f(t)$ is the functional representation of the curve in Figure 1. Although the temperature field is non-axisymmetric, it is readily seen from (1) that the field is symmetric with respect to θ . Since the temperature equation is needed for the development of the stress equations, it is convenient to rewrite (1) as

$$T(r, \theta, t) = T_0 + \frac{2H_0}{\pi \rho c r_0} \left\{ A_{00}(t) + \sum_{m=0}^{\infty} \sum_{n=1}^{\infty} A_{mn}(t) J_m(\lambda_{mn} r) \cos m\theta \right\} \quad (2)$$

where

$$A_{00}(t) = \int_0^t f(t') dt' \quad (3)$$

$$A_{on}(t) = \frac{e^{-\lambda_{on}^2 \frac{\kappa}{\rho c} t}}{J_0(\lambda_{on} r_0)} \int_0^t e^{\lambda_{on}^2 \frac{\kappa}{\rho c} t'} f(t') dt' \quad (4)$$

$$A_{1n}(t) = \frac{\pi [\lambda_{1n} r_0]^2 e^{-\lambda_{1n}^2 \frac{\kappa}{\rho c} t}}{2 [(\lambda_{1n} r_0)^2 - 1] J_1(\lambda_{1n} r_0)} \int_0^t e^{\lambda_{1n}^2 \frac{\kappa}{\rho c} t'} f(t') dt' \quad (5)$$

and

$$A_{mn}(t) = - \frac{2 [\lambda_{mn} r_0]^2 \cos \left(\frac{m \pi}{2} \right) e^{-\lambda_{mn}^2 \frac{\kappa}{\rho c} t}}{[m^2 - 1] [(\lambda_{mn} r_0)^2 - m^2] J_m(\lambda_{mn} r_0)} \times \int_0^t e^{\lambda_{mn}^2 \frac{\kappa}{\rho c} t'} f(t') dt' \quad (6)$$

for $m \geq 2$.

III. STRESS EQUATIONS

Under the plane strain assumption, the stresses in the cylinder can be determined from the following formulae³:

$$T_{rr} = \left\{ \frac{1}{r} \frac{\partial}{\partial r} + \frac{1}{r^2} \frac{\partial^2}{\partial \theta^2} \right\} \left\{ \Omega_1(r, \theta, t) - 2G \Omega_2(r, \theta, t) \right\} \quad (7)$$

$$T_{r\theta} = - \frac{\partial^2}{\partial \theta \partial r} \left[\frac{1}{r} \left\{ \Omega_1(r, \theta, t) - 2G \Omega_2(r, \theta, t) \right\} \right] \quad (8)$$

$$T_{\theta\theta} = \frac{\partial^2}{\partial r^2} \left\{ \Omega_1(r, \theta, t) - 2G \Omega_2(r, \theta, t) \right\} \quad (9)$$

and

$$T_{zz} = \nu (T_{rr} + T_{\theta\theta}) - 2G(1 + \nu) \alpha \Phi(r, \theta, t) \quad (10)$$

where Ω_1 is the solution of the biharmonic equation,

$$\Delta^2 \Delta^2 \Omega_1 = 0 \quad (11)$$

³

W. Nowacki, *Thermoelasticity*, Addison-Wesley Publishing Company, Inc., Reading, Massachusetts, 1962, p. 389.

$$\Omega_2 \text{ is a particular solution of } \Delta^2 \Omega_2 = \left(\frac{1 + \nu}{1 - \nu} \right) \alpha \Phi \quad (12)$$

and Φ is the change in the temperature field. A solution of (11)⁴ which is well behaved at $r=0$ and is symmetric with respect to θ is

$$\Omega_1 = b_0 r^2 + \sum_{\ell=1}^{\infty} \left[(a_{\ell} r^{\ell} + b_{\ell} r^{\ell+2}) \cos \ell \theta + (c_{\ell} r^{\ell} + d_{\ell} r^{\ell+2}) \sin \ell \theta \right] \quad (13)$$

and a particular solution of (12)⁵ is

$$\Omega_2 = \left(\frac{1 + \nu}{1 - \nu} \right) \frac{\alpha \kappa}{\rho c} \int_{t_i}^t \Phi dt \quad (14)$$

when the initial temperature or the final temperature is uniform.

Since the initial temperature and the final temperature of the cylinder is uniform, we can define Φ as either $T(t) - T(0)$ or $T(t) - T(\infty)$. By choosing the latter and allowing $f(t')=0$ for $t' > t$,

$$\int_{t_s}^t \Phi dt = - \frac{2H_0}{\pi \kappa r_0} \sum_{m=0}^{\infty} \sum_{n=1}^{\infty} \frac{A_{mn}(t)}{\lambda_{mn}^2} J_m(\lambda_{mn} r) \cos m \theta \quad (15)$$

and

$$\Omega_2 = - \frac{2\alpha H_0}{\pi \rho c r_0} \left(\frac{1 + \nu}{1 - \nu} \right) \sum_{m=0}^{\infty} \sum_{n=1}^{\infty} \frac{A_{mn}(t)}{\lambda_{mn}^2} J_m(\lambda_{mn} r) \cos m \theta \quad (16)$$

The substitution of (13) and (16) into (7) through (10) results in

$$\begin{aligned} T_{rr} = & 2b_0 + 2b_1 r \cos \theta + \sum_{m=2}^{\infty} \left[(m-m^2) a_m r^{m-2} + (2 + m-m^2) b_m r^m \right] \cos m \theta \\ & + 2G \left\{ \frac{2\alpha H_0}{\pi \rho c r_0} \left(\frac{1 + \nu}{1 - \nu} \right) \sum_{m=0}^{\infty} \sum_{n=1}^{\infty} \left[\frac{J'_m(\lambda_{mn} r)}{\lambda_{mn} r} - m^2 \frac{J_m(\lambda_{mn} r)}{(\lambda_{mn} r)^2} A_{mn}(t) \right] \cos m \theta \right\} \end{aligned} \quad (17)$$

⁴ Y.C. Fung, *Foundations of Solid Mechanics*, Prentice-Hall, Inc., Englewood, Cliffs, New Jersey, 1965, p. 246.

⁵ B.A. Boley and J.H. Weiner, *Theory of Thermal Stresses*, John Wiley & Sons, Inc., New York, New York, 1960, p. 83.

$$\begin{aligned}
T_{r\theta} = & 2b_1 r \sin \theta + \sum_{m=2}^{\infty} \left[(m^2 - m) a_m r^{m-2} + (m^2 + m) b_m r^m \right] \sin m \theta \\
& + 2G \left\{ \frac{2\alpha H_0}{\pi \rho c r_0} \left(\frac{1+\nu}{1-\nu} \right) \sum_{m=0}^{\infty} \sum_{n=1}^{\infty} m \left[\frac{J'_m(\lambda_{mn} r)}{\lambda_{mn} r} - \frac{J_m(\lambda_{mn} r)}{(\lambda_{mn} r)^2} \right] A_{mn}(t) \sin m \theta \right\}
\end{aligned} \tag{18}$$

$$\begin{aligned}
T_{\theta\theta} = & 2b_0 + 6b_1 r \cos \theta + \sum_{m=2}^{\infty} \left[(m^2 - m) a_m r^{m-2} + (m^2 + 3m + 2) b_m r^m \right] \cos m \theta \\
& + \frac{4\alpha G H_0}{\pi \rho c r_0} \left(\frac{1+\nu}{1-\nu} \right) \sum_{m=0}^{\infty} \sum_{n=1}^{\infty} A_{mn}(t) J_m(\lambda_{mn} r) \cos m \theta
\end{aligned} \tag{19}$$

and

$$\begin{aligned}
T_{zz} = & \nu (T_{rr} + T_{\theta\theta}) - \frac{4\alpha G H_0}{\pi \rho c r_0} (1 + \nu) \sum_{m=0}^{\infty} \sum_{n=1}^{\infty} A_{mn}(t) \\
& \times J_m(\lambda_{mn} r) \cos m \theta
\end{aligned} \tag{20}$$

Since the cylinder is unrestrained, the stresses at the surface must satisfy

$$T_{rr}(r_0, \theta, t) = T_{r\theta}(r_0, \theta, t) = 0 \tag{21}$$

By substituting (21) into (17) and (18) one obtains

$$0 = 2b_0 + 2b_1 r_0 \cos \theta + \sum_{\ell=2}^{\infty} \left[(\ell - \ell^2) a_{\ell} r_0^{\ell-2} + (2 + \ell + \ell^2) b_{\ell} r_0^{\ell} \right]$$

$$\cos \ell \theta + 2G \left\{ \frac{2\alpha H_0}{\pi \rho c r_0} \left(\frac{1+\nu}{1-\nu} \right) \sum_{m=0}^{\infty} \sum_{n=1}^{\infty} \frac{J'_m(\lambda_{mn} r_0)}{\lambda_{mn} r_0} \right.$$

$$\left. - m^2 \frac{J_m(\lambda_{mn} r_0)}{(\lambda_{mn} r_0)} A_{mn}(t) \cos m \theta \right\} \quad (22)$$

and

$$0 = 2b_1 r_0 \sin \theta + \sum_{\ell=2}^{\infty} \left[(\ell^2 - \ell) a_{\ell} r_0^{\ell-2} + (\ell^2 + \ell) b_{\ell} r_0^{\ell} \right] \sin \ell \theta$$

$$+ 2G \left\{ \frac{2\alpha H_0}{\pi \rho c r_0} \left(\frac{1+\nu}{1-\nu} \right) \sum_{m=0}^{\infty} \sum_{n=1}^{\infty} m \left[\frac{J'_m(\lambda_{mn} r_0)}{\lambda_{mn} r_0} - \frac{J_m(\lambda_{mn} r_0)}{(\lambda_{mn} r_0)^2} \right] A_{mn}(t) \sin m \theta \right\} \quad (23)$$

where $J'_m(\lambda_{mn} r_0) = 0^*$

Equations (22) and (23) will be satisfied for all values of ℓ , m , and n if

$$\ell = m \quad (24)$$

$$b_0 = 0 \quad (25)$$

$$b_1 = \frac{2\alpha H_0}{\pi \rho c r_0} \left(\frac{1+\nu}{1-\nu} \right) \sum_{n=1}^{\infty} \frac{J_1(\lambda_{1n} r_0)}{\lambda_{1n} r_0} A_{1n}(t) \quad (26)$$

and

$$(m^2 - m) r_0^{m-2} a_m + (m^2 - m) r_0^m b_m = \frac{4G\alpha H_0}{\pi \rho c r_0} \left(\frac{1+\nu}{1-\nu} \right) m \sum_{n=1}^{\infty} \frac{J_m(\lambda_{mn} r_0)}{(\lambda_{mn} r_0)^2} A_{mn}(t) \quad (27)$$

* This is a consequence of satisfying the boundary conditions in the deviation of the temperature field equation.

$$\text{and } (m-m^2)r_0^{m-2}a_m + (2+m-m^2)r_0^m b_m = \frac{4G\alpha H_0}{\Pi\rho c r_0} \left(\frac{1+\nu}{1-\nu} \right) \times m^2 \sum_{n=1}^{\infty} \frac{J_m(\lambda_{mn}r_0)}{(\lambda_{mn}r_0)^2} A_{mn}(t) \quad (28)$$

for $m \geq 2$. The simultaneous solution of (27) and (28) yields

$$a_m = \frac{2G\alpha H_0}{\Pi\rho c r_0^{m-2}} \left(\frac{1+\nu}{1-\nu} \right) (2+m) \sum_{n=1}^{\infty} \frac{J_m(\lambda_{mn}r_0)}{(\lambda_{mn}r_0)^2} A_{mn}(t) \quad (29)$$

and

$$b_m = \frac{2G\alpha H_0}{\Pi\rho c r_0^{m+1}} \left(\frac{1+\nu}{1-\nu} \right) m \sum_{n=1}^{\infty} \frac{J_m(\lambda_{mn}r_0)}{(\lambda_{mn}r_0)^2} A_{mn}(t) \quad (30)$$

for $m \geq 2$.

Both the temperature and stress equations, (2), (17), (18), (19), and (20), can be reduced to a dimensionless form through the use of the following dimensionless quantities:

$$\left. \begin{aligned} r^* &= \frac{r}{r_0} & t^* &= \frac{t}{t_0} & \rho_{mn} &= \lambda_{mn} r_0 \\ \beta^* &= \frac{\kappa t_0}{\rho c r_0^2} & T^* &= \frac{T - T_0}{0.24 \frac{Q}{\rho c r_0}} \\ a_m^* &= \frac{a_m}{0.24 \frac{\alpha G Q}{\rho c r_0} \left(\frac{1+\nu}{1-\nu} \right)} & b_m^* &= \frac{b_m}{0.24 \frac{\alpha G Q}{\rho c r_0} \left(\frac{1+\nu}{1-\nu} \right)} \\ T_{ij}^* &= \frac{T_{ij}}{0.24 \frac{\alpha G Q}{\rho c r_0} \left(\frac{1+\nu}{1-\nu} \right)} & i, j &= r, \theta, z \end{aligned} \right\} (31)$$

The use of these quantities yields

$$T^* = A_{00}(t^*) + \sum_{m=0}^{\infty} \sum_{n=1}^{\infty} A_{mn}(t^*) J_m(\rho_{mn} r^*) \cos m \theta \quad (32)$$

$$T_{rr}^* = 2b_1^* r^* \cos \theta + \sum_{m=2}^{\infty} \left[(m-m^2) a_m^*(r^*)^{m-2} + (2+m-m^2) \right. \\ \left. \times b_m^*(r^*)^m \right] \cos m \theta + 2 \sum_{m=0}^{\infty} \sum_{n=1}^{\infty} \left[\frac{J_m'(\rho_{mn} r^*)}{\rho_{mn} r^*} - m^2 \frac{J_m(\rho_{mn} r^*)}{(\rho_{mn} r^*)^2} \right] A_{mn}(t^*) \cos m \theta \quad (33)$$

$$T_{r\theta}^* = 2b_1^* r^* \sin \theta + \sum_{m=2}^{\infty} \left[(m-m^2) a_m^*(r^*)^{m-2} - (m^2+m) b_m^*(r^*)^m \right] \\ \times \sin m \theta + 2 \sum_{m=1}^{\infty} \sum_{n=1}^{\infty} m \left[\frac{J_m'(\rho_{mn} r^*)}{\rho_{mn} r^*} - \frac{J_m(\rho_{mn} r^*)}{(\rho_{mn} r^*)} \right] A_{mn}(t^*) \sin m \theta \quad (34)$$

$$T_{\theta\theta}^* = 6b_1^* r^* \cos \theta + \sum_{m=2}^{\infty} \left[(m^2-m) a_m^*(r^*)^{m-2} \right. \\ \left. + (m^2+3m+2) b_m^*(r^*)^m \right] \cos m \theta + 2 \sum_{m=0}^{\infty} \sum_{n=1}^{\infty} A_{mn}(t^*) J_m''(\rho_{mn} r^*) \cos m \theta \quad (35)$$

$$T_{zz}^* = \nu(T_{rr}^* + T_{\theta\theta}^*) - 2(1-\nu) \sum_{m=0}^{\infty} \sum_{n=1}^{\infty} A_{mn}(t^*) J_m(\rho_{mn} r^*) \cos m \theta \quad (36)$$

IV. PARAMETRIC ANALYSIS

The values of the non-dimensional temperatures and stresses were calculated for $\beta^* = 0.01, 0.1, \text{ and } 1.0$; for $t^* = 1.0 \text{ and } 10.0$; and for $\theta = 0, \frac{\pi}{2}, \pi, \text{ and } \frac{3\pi}{2}$. Because v appears in the right hand side of (36), $v = 0.33$ was used² in calculating T_{zz}^* . Figures 2,3 and 4 are the plots of the temperature distributions and Figures 5 through 14 are the plots of the stress distributions.

For a given material of a given radius, the influence of β^* (and consequently, t_o^*) and Q on the temperature field can be seen from Figures 2,3 and 4. At $t^* = 1.0$ and $t^* = 10.0$, the surface temperature for $\theta = 0$ decreases as β^* increases if Q remains constant. For $\theta = \frac{\pi}{2}$ and consequently, $\frac{3\pi}{2}$, the surface temperature increases as β^* increases at $t^* = 1.0$ and $t^* = 10.0$. It can be concluded from Figures 3 and 4 that, for $\beta^* \neq 1.0$, the temperature in the cylinder is uniform for all values of Q . For a given β^* , it follows from (31) that the temperature at any point in the cylinder will increase as Q increases and will decrease as Q decreases.

The effect of β^* and Q on the thermal stresses at $t^* = 1.0$ and $t^* = 10.0$ can be seen from Figures 5 through 14. Except for T_{rr}^* on $\theta = \frac{\pi}{2}$ and $\theta = \frac{3\pi}{2}$ (See Figure 8), an increase in β^* results in a decrease in stresses if Q remains constant. Since the lateral surface of the cylinder is traction free, T_{rr}^* and $T_{r\theta}^*$ are zero for $r_o = 1$. Consequently the maximum value of these stresses occurs at an interior point of the cylinder as is shown in Figures 5, 10 and 12. In addition to influencing the maximum value of these stresses, β^* also effects the location of the maximum value. At $t^* = 1.0$ and $t^* = 10.0$, an increase in β^* shifts the maximum value of T_{rr}^* towards the rear lateral surface of the cylinder (See Figures 5 and 12); and an increase in β^* shifts the maximum values of $T_{r\theta}^*$ towards the center of the cylinder (See Figure 10). As in the case of the temperature distribution, it follows from (33), (34), (35) and (36) that, for a given β^* , the stresses at any point in the cylinder will increase as Q increases and will decrease as Q decreases.

Using simple beam theory, this author⁵ had shown that the maximum axial stress in simply supported rectangular beams exposed to a nuclear thermal environment did not occur at $t^* = 1.0$ but at some later t^* .

⁵ E.F. Quigley, "Thermoelastic Response of Aluminum Alloy Beams and Plates Exposed to Nuclear Thermal Environments", BRL-MR 2427, December 1974, US Army Ballistic Research Laboratory, Aberdeen Proving Ground, MD 21005. (AD #B001134L)

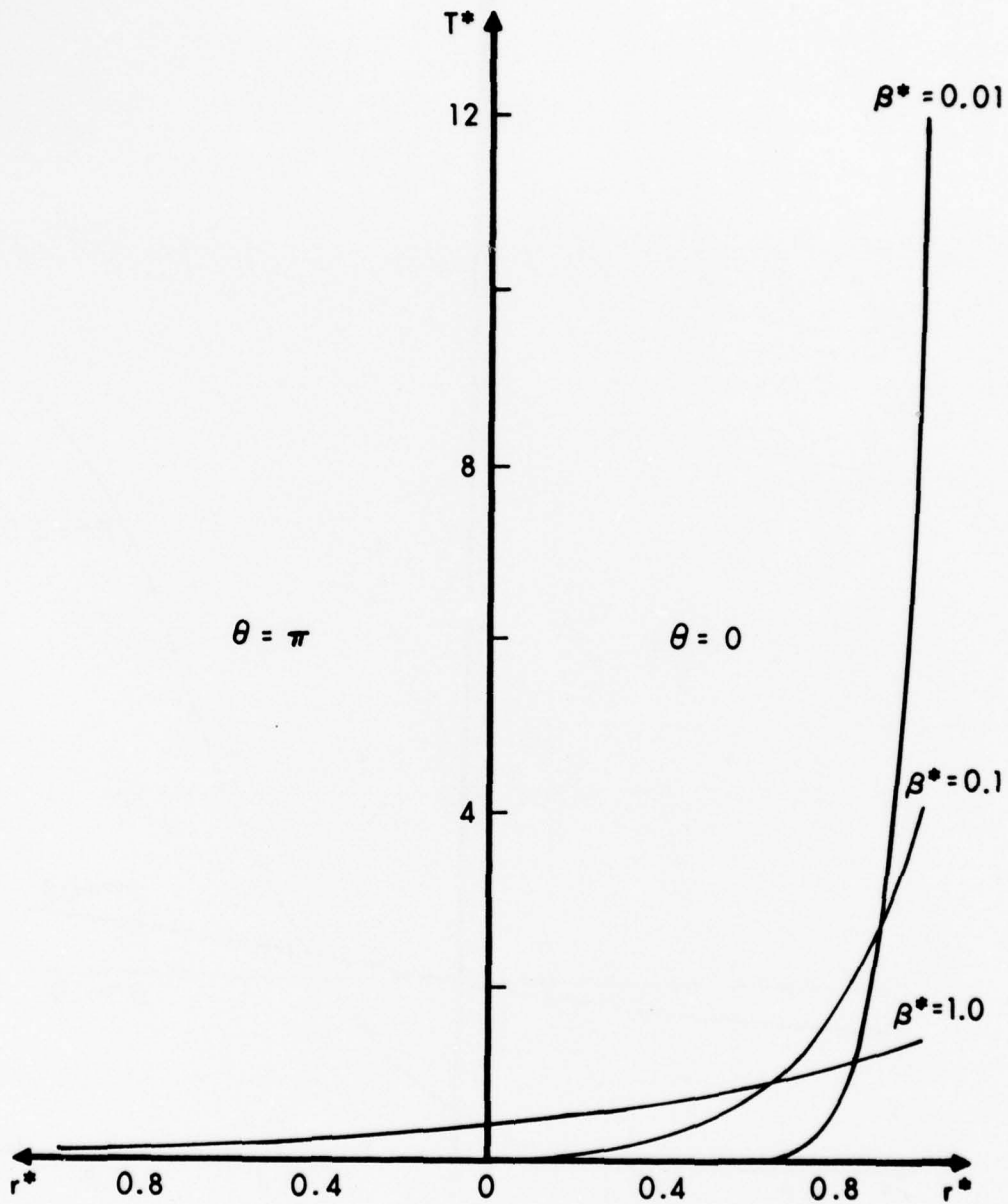


Figure 2. Radial Temperature Distribution on $\theta = 0$ and π for $t^* = 1.0$ and $\beta^* = 0.01, 0.1,$ and 1.0

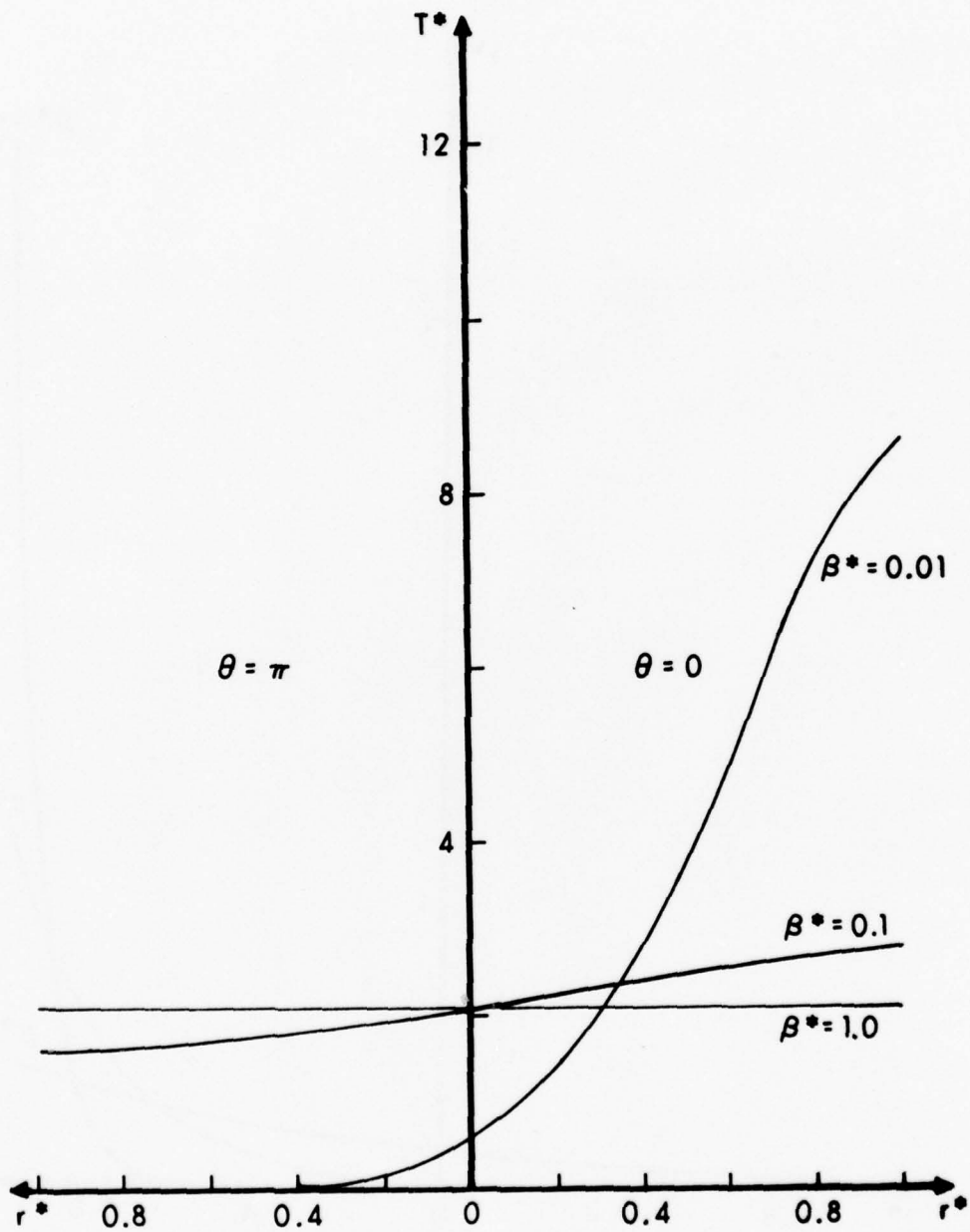


Figure 5. Radial Temperature Distribution on $\theta = 0$ and π for $t^* = 10.0$ and $\beta^* = 0.01, 0.1, \text{ and } 1.0$

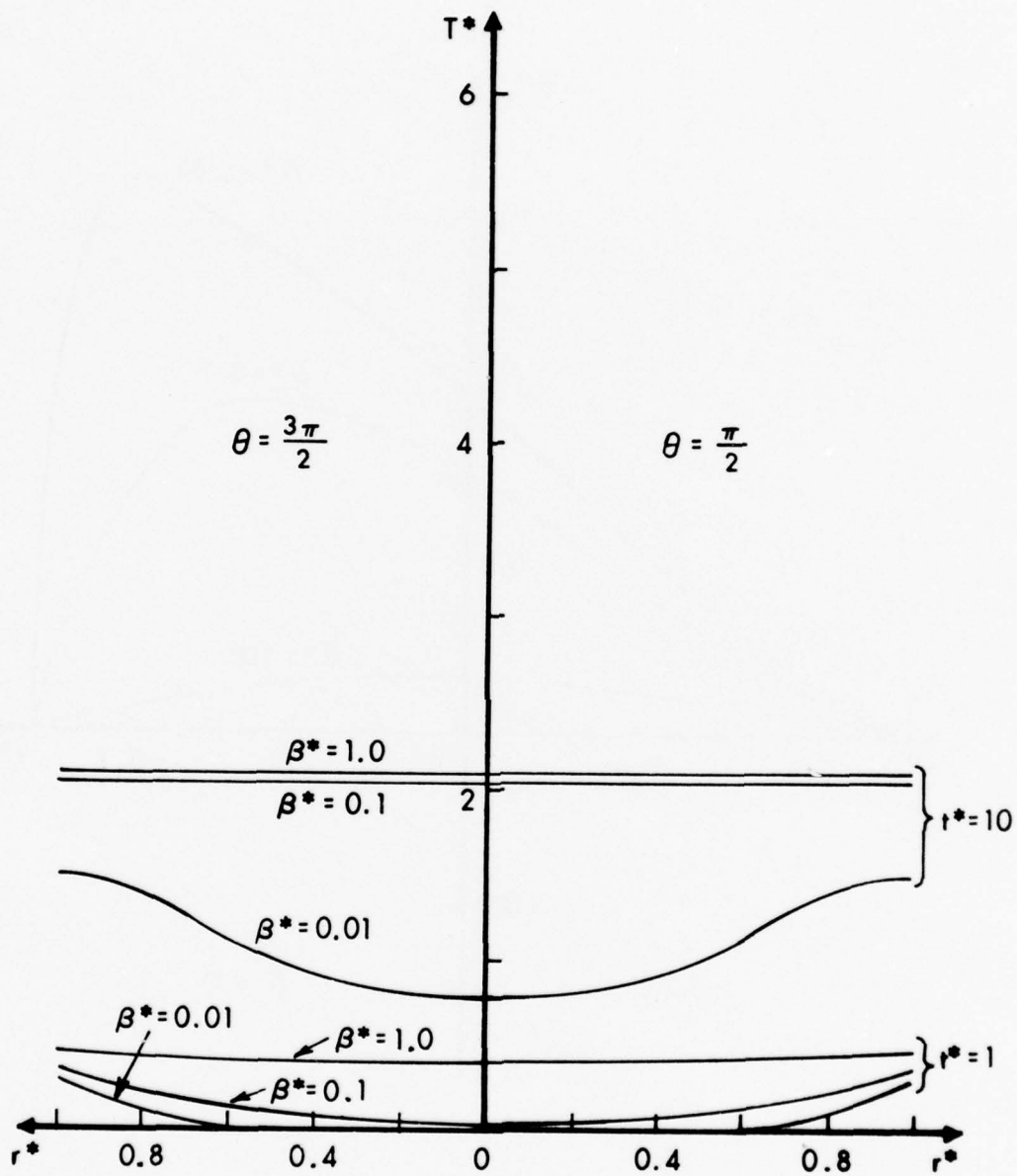


Figure 4. Radial Temperature Distribution on $\theta = \frac{\pi}{2}$ and $\frac{3\pi}{2}$
 for $t^* = 1.0$ and 10.0 and $\beta^* = 0.01, 0.1,$ and 1.0

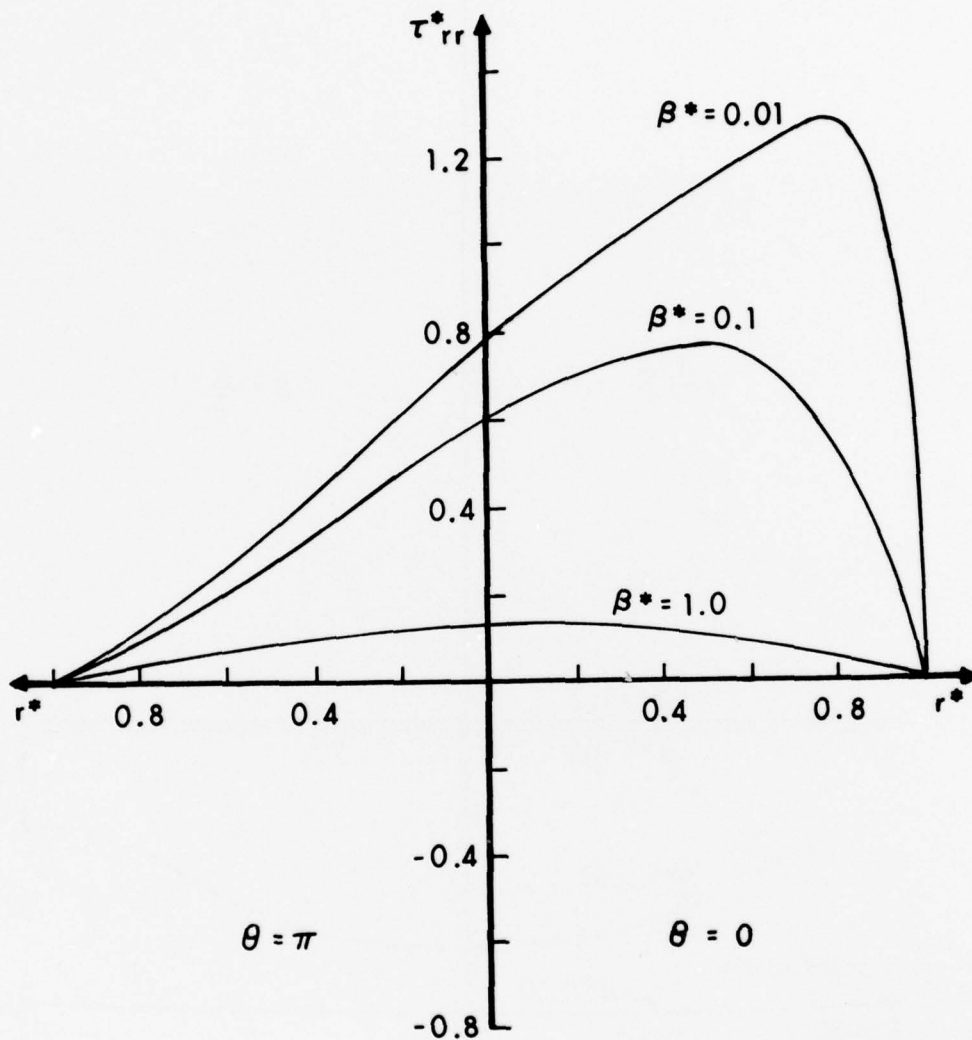


Figure 5. Radial Stress Distribution on $\theta = 0$ and π for $t^* = 1.0$ and $\beta^* = 0.01, 0.1, \text{ and } 1.0$

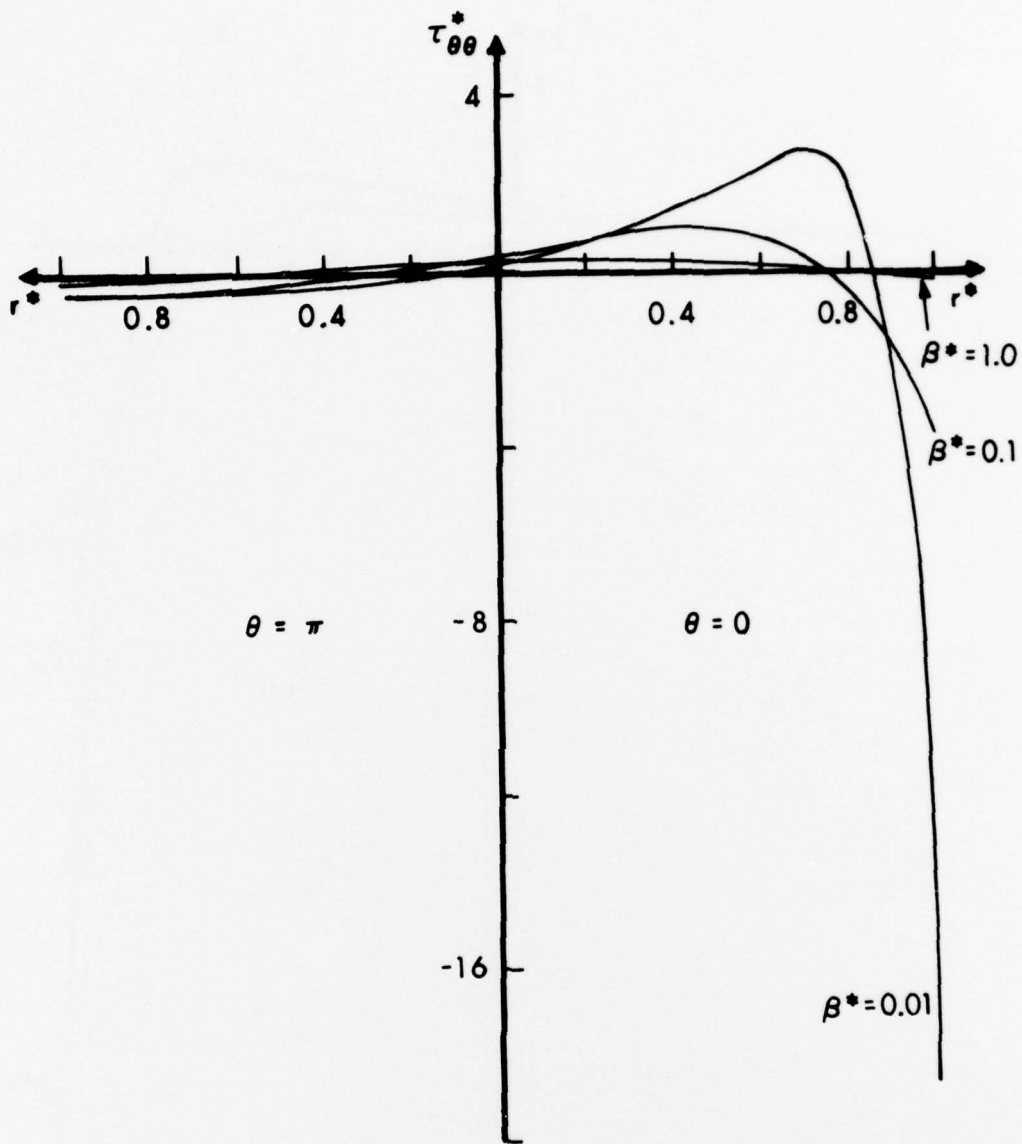


Figure 6. Tangential Stress Distribution on $\theta = 0$ and π for $\tau^* = 1.0$ and $\beta^* = 0.01, 0.1, \text{ and } 1.0$

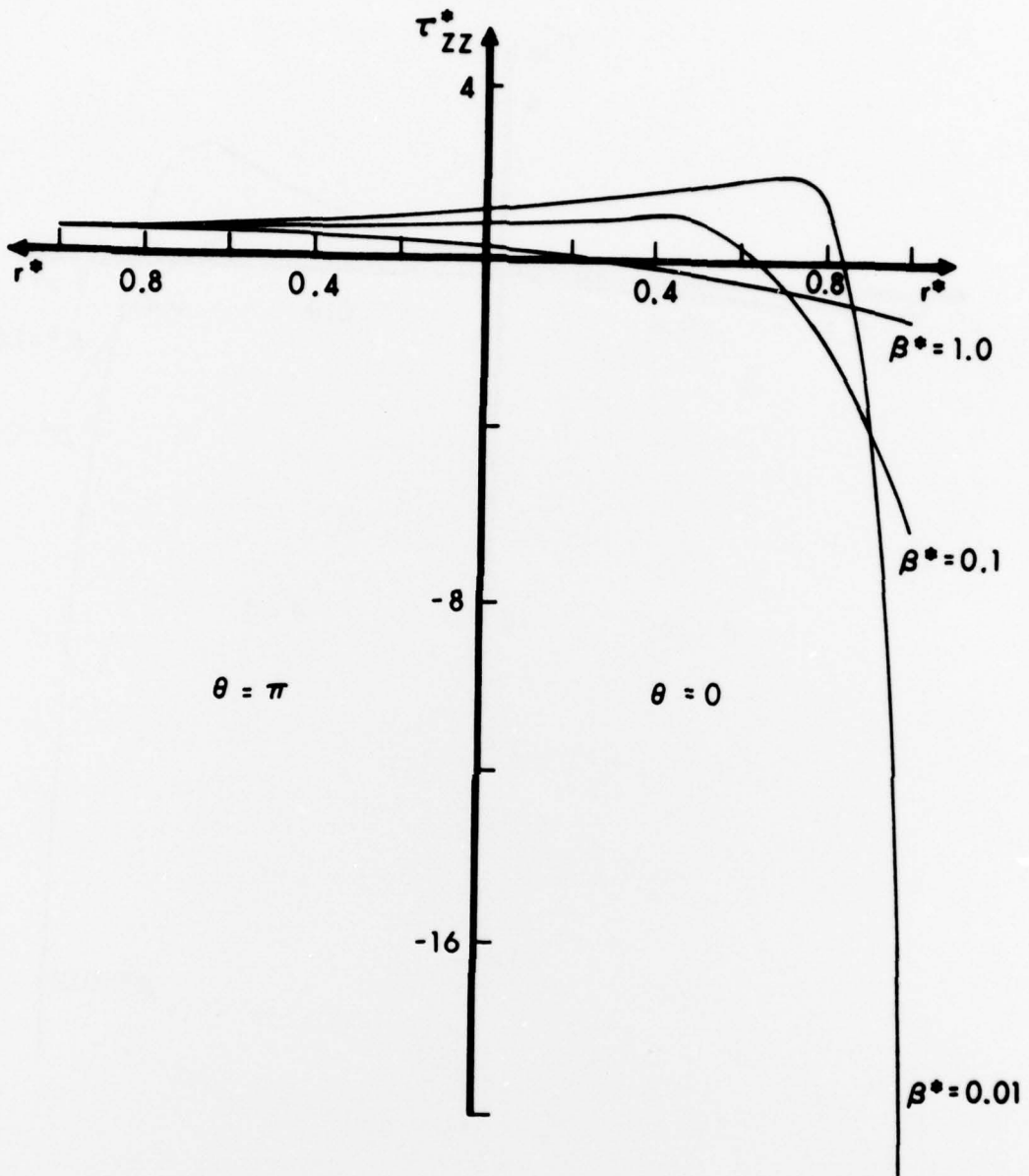


Figure 7. Axial Stress Distribution on $\theta = 0$ and π for $t^* = 1.0$ and $\beta^* = 0.01, 0.1, \text{ and } 1.0$

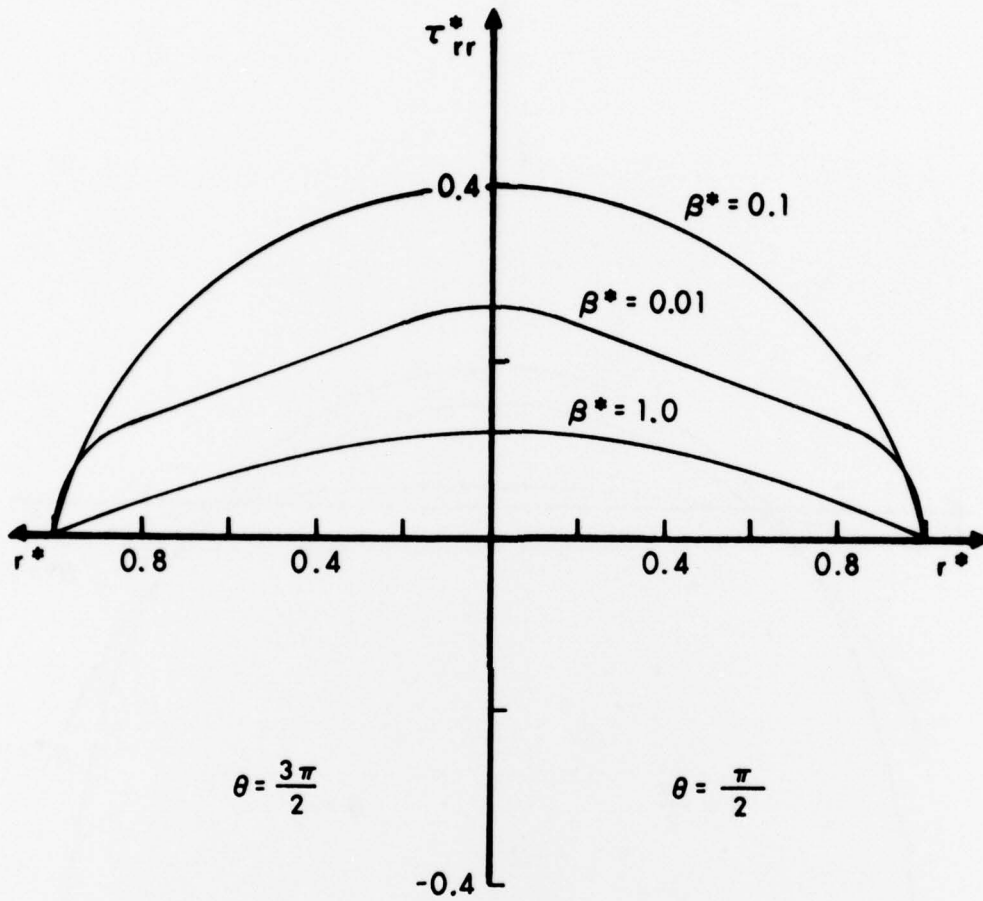


Figure 8. Radial Stress Distribution on $\theta = \frac{\pi}{2}$ and $\frac{3\pi}{2}$
for $t^* = 1.0$ and $\beta^* = 0.01, 0.1, \text{ and } 1.0$

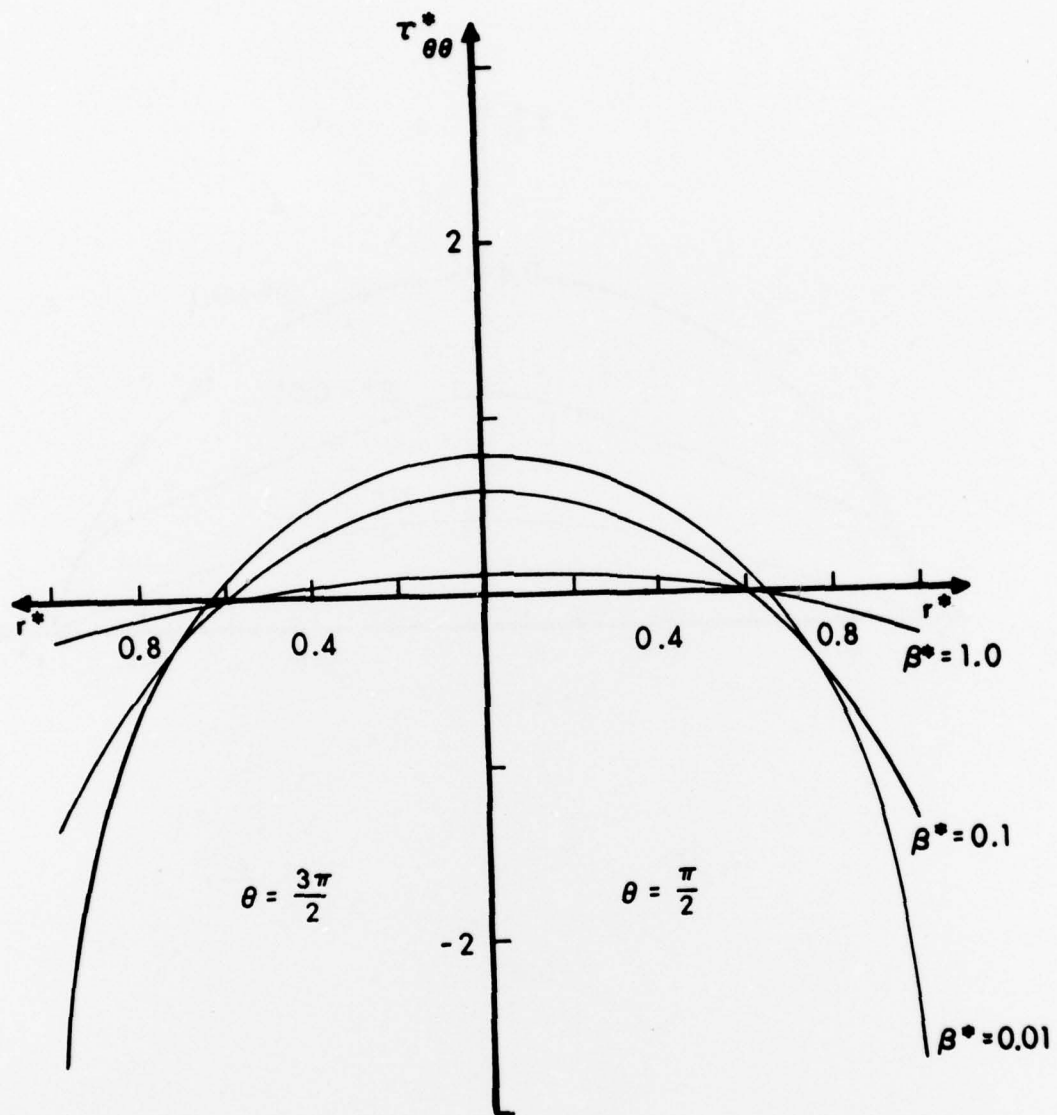


Figure 9. Tangential Stress Distribution on $\theta = \frac{\pi}{2}$ and $\frac{3\pi}{2}$ for $t^* = 1.0$ and $\beta^* = 0.01, 0.1,$ and 1.0

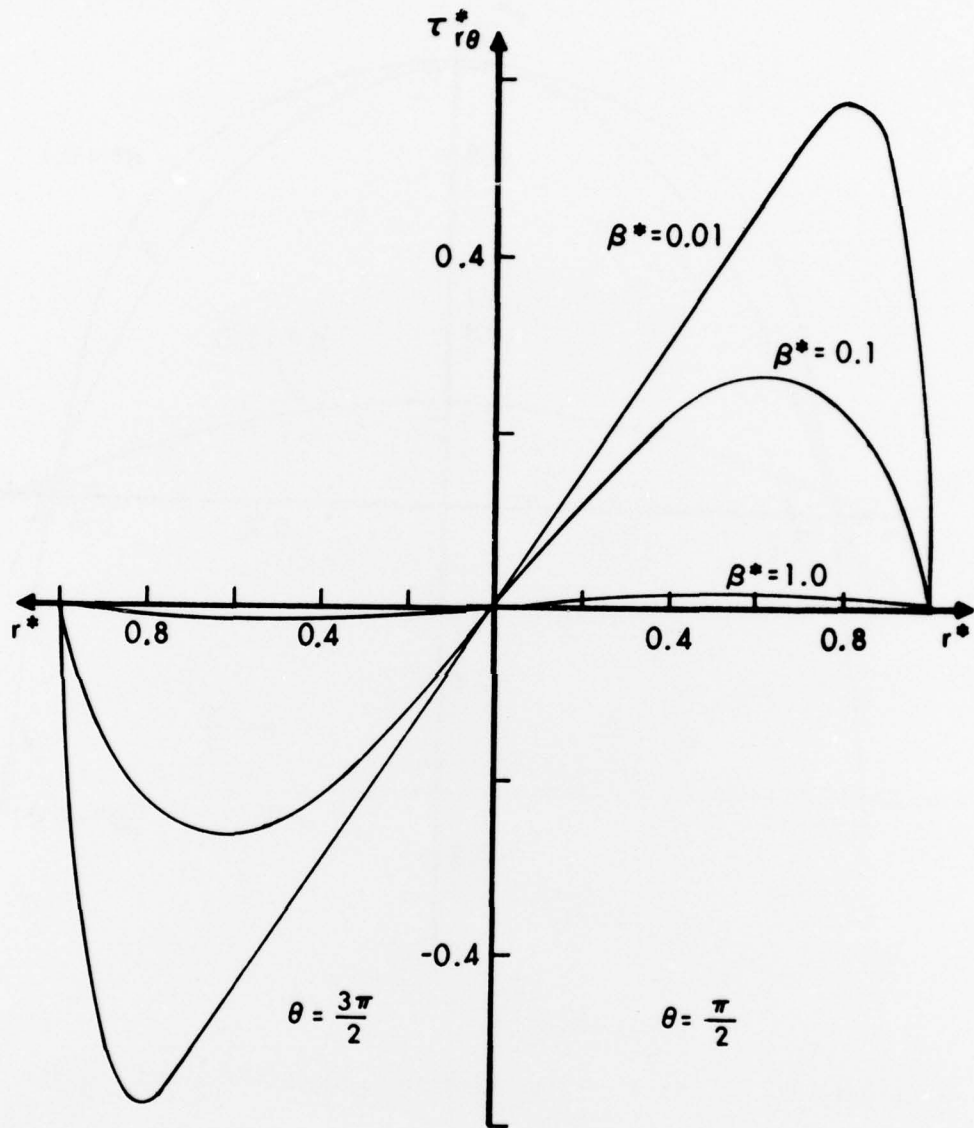


Figure 10. Shear Stress Distribution on $\theta = \frac{\pi}{3}$ and $\frac{3\pi}{2}$ for $t^* = 1.0$ and $\beta^* = 0.01, 0.1,$ and 1.0

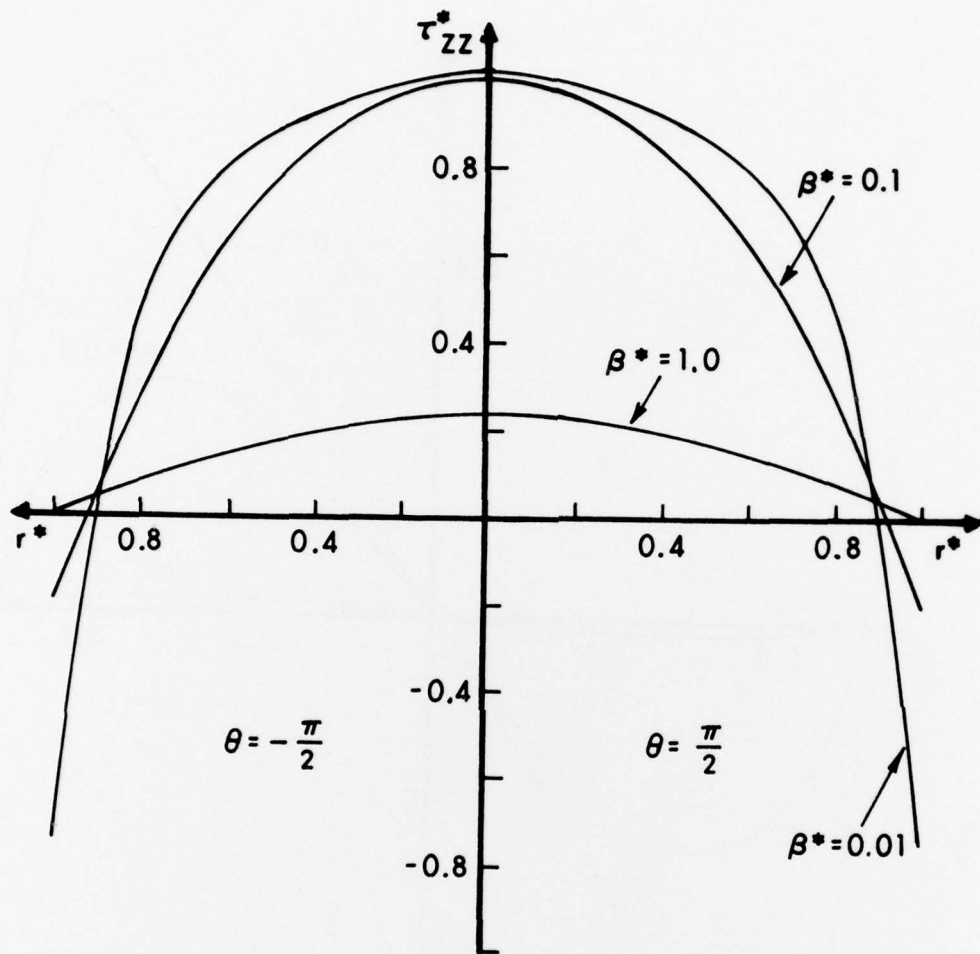


Figure 11. Axial Stress Distribution on $\theta = \frac{\pi}{2}$ and $-\frac{\pi}{2}$ for $T^* = 1.0$ and $\beta^* = 0.01, 0.1$ and 1.0

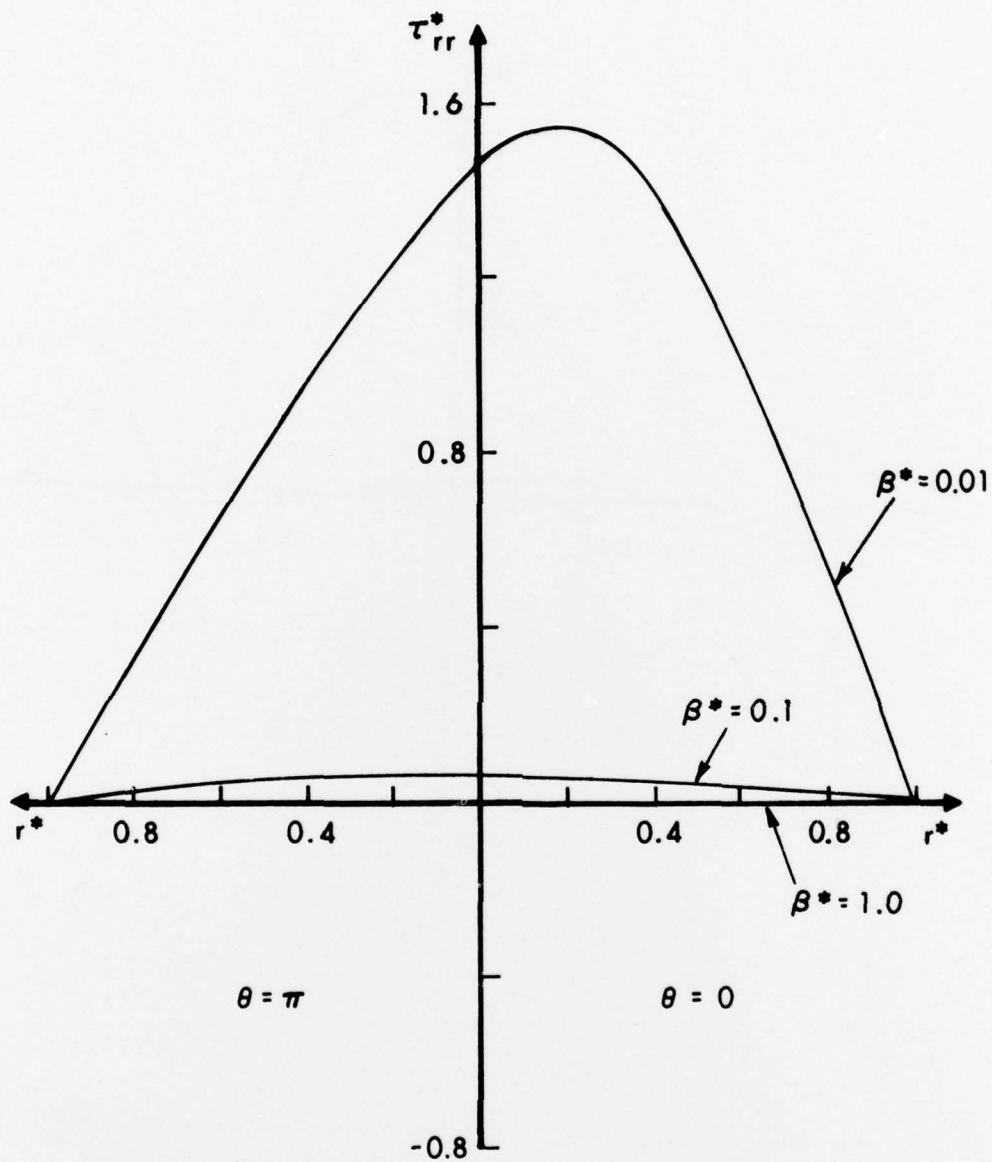


Figure 12. Radial Stress Distribution on $\theta = 0$ and π for $t^* = 10.0$ and $\beta^* = 0.01, 0.1, \text{ and } 1.0$

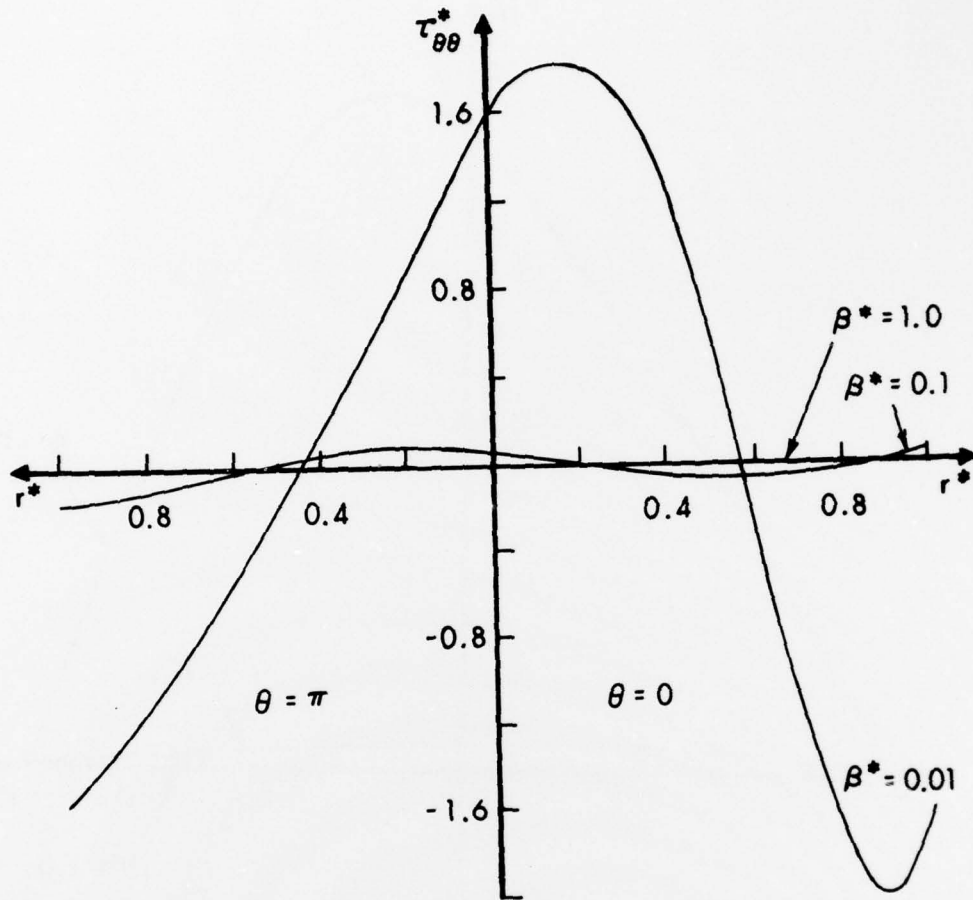


Figure 13. Tangential Stress Distribution on $\theta = 0$ and π for $t^* = 10.0$ and $\beta^* = 0.01, 0.1,$ and 1.0

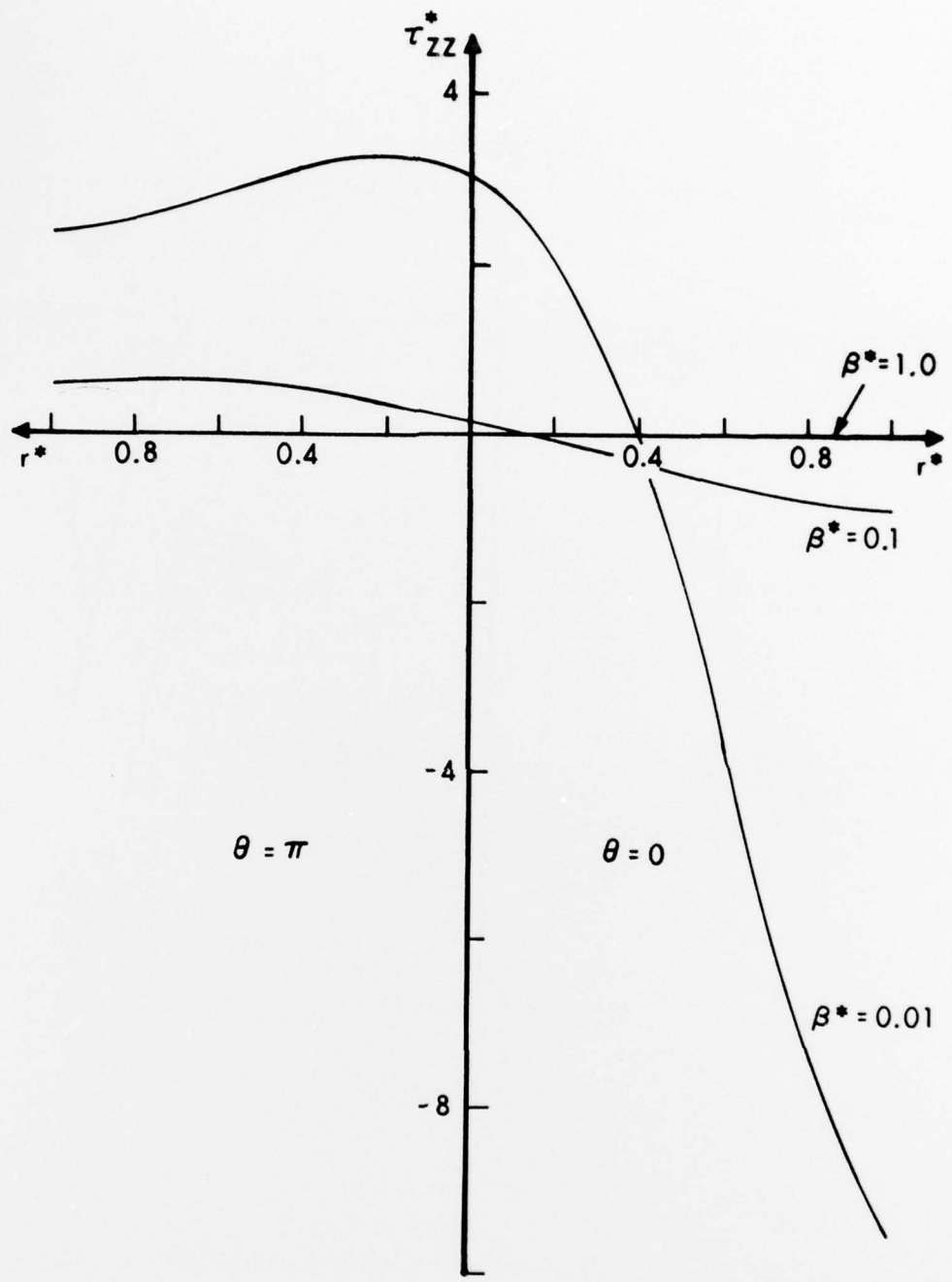


Figure 11. Axial Stress Distribution on $\theta = 0$ and π for $t^* = 10.0$ and $\beta^* = 0.01, 0.1, \text{ and } 1.0$

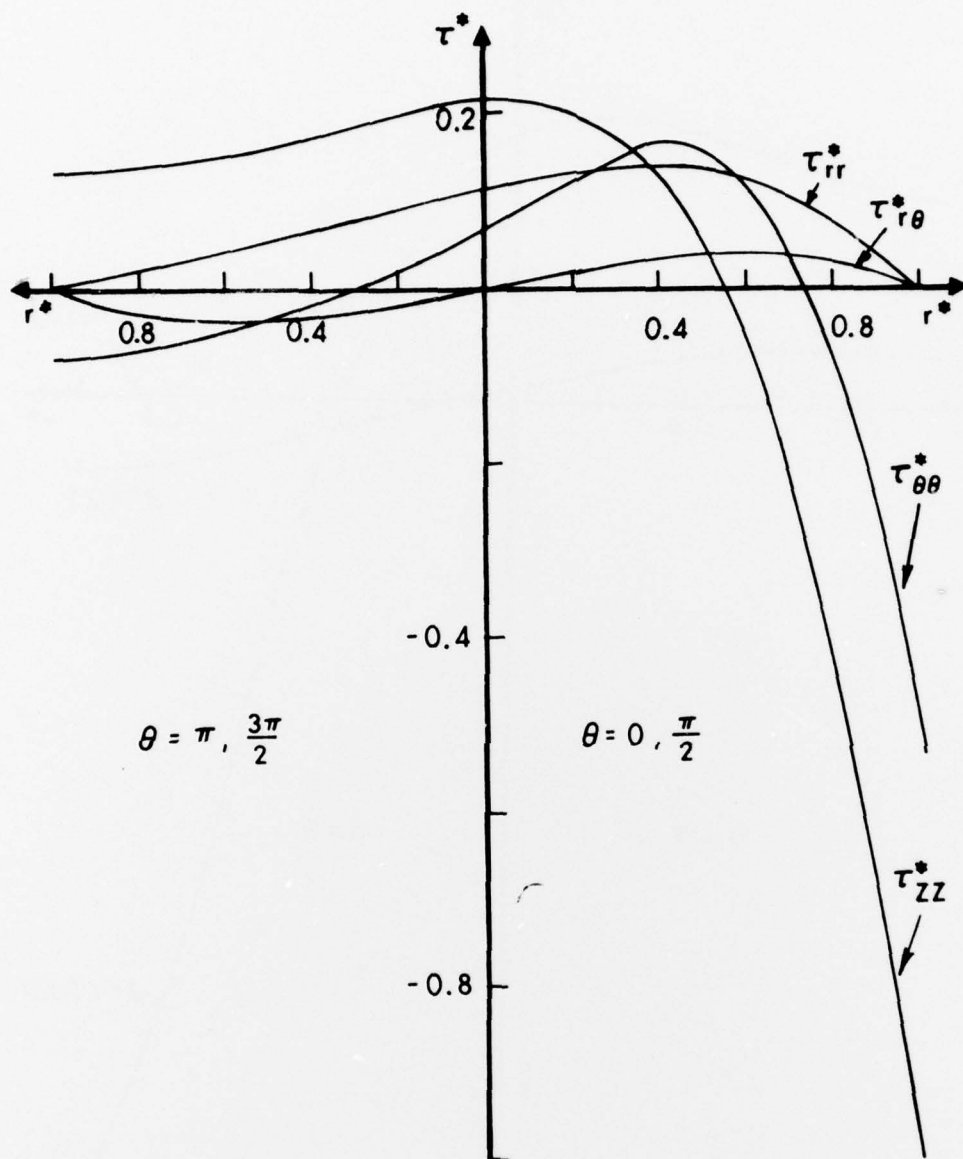


Figure 15. Normalized T_{rr}^* , $T_{\theta\theta}^*$, and T_{zz}^* on $\theta = 0$ and π and Normalized $T_{r\theta}^*$ on $\theta = \frac{\pi}{2}$ and $\frac{3\pi}{2}$ at the Time of their Maximum Value for $B^* = 0.1$

By trial and error, it was determined for $\beta^* = 0.1$ that maximum value of T_{rr}^* , $T_{r\theta}^*$, and T_{zz}^* occurred at $t^* = 1.35$ and that the maximum value of $T_{\theta\theta}^*$ occurred at $t^* = 1.10$. Figure 15 is a composite plot of T_{rr}^* , $T_{\theta\theta}^*$, T_{zz}^* and $T_{r\theta}^*$, normalized to the maximum value of T_{zz}^* , at the time of their maximum value. It is seen from Figure 15 that the maximum values of T_{rr}^* and $T_{r\theta}^*$ are small compared to the maximum value of T_{zz}^* . However, it is seen from this figure that the maximum value of $T_{\theta\theta}^*$ is not small compared to the maximum value of T_{zz}^* ; the latter being only twice as large as the former. Also, it can be seen that the axial stress is the largest compression stress and the largest tension stress.

V. CONCLUSION

A set of non-dimensional equations for the quasi-static, thermal stress field in a long, unrestrained, isotropic, homogeneous, solid cylinder whose lateral surface is subjected to heating by a nuclear thermal environment have been derived under the plane strain assumption. The results of a parametric analysis of the stress field involving the rise time of the thermal pulse, t_0 , and the total energy of the thermal environment, Q , shows:

1. For a given Q , an increase in t_0 results in a decrease in the maximum value of the stress
2. For a given Q , an increase in t_0 shifts the location of the maximum value of the stress for those stresses which are zero on the lateral surface of the cylinder, and
3. For a given t_0 , the stresses at any point in the cylinder will increase as Q increases and will decrease as Q decreases.

GLOSSARY OF TERMS

a_m	= Coefficients defined by (29)
a_m^*	= Dimensionless variable defined by (31)
b_m	= Coefficients defined by (30)
b_m^*	= Dimensionless variable defined by (31)
c	= Specific heat
$f(t)$	= Time dependent portion of curve in Figure 1
r	= Radial coordinate
r_0	= Radius of cylinder
r^*	= Dimensionless variable defined by (31)
t	= Time
t'	= Dummy integration variable
t_0	= Rise time of thermal pulse
t^*	= Dimensionless variable defined by (31)
A_{mn}	= Coefficients defined by (3) through (6)
G	= Shear modulus
$H, H(t)$	= $H_0 f(t)$
H_0	= Maximum irradiance of nuclear thermal pulse
$J_m(u)$	= Ordinary Bessel function of argument u
$J'_m(u)$	= $\frac{dJ_m(u)}{du}$
Q	= $\int_0^{\infty} H(t) dt$
$T, T(r, \theta, t)$	= Temperature in cylinder
T_0	= Initial temperature in cylinder
α	= Coefficient of linear expansion
β^*	= Dimensionless variable defined by (31)
θ	= Angular coordinate
κ	= Thermal conductivity
$\lambda_{mn} r_0$	= The n -th positive roots of $J'_m(\lambda_{mn} r_0) = 0$
ν	= Poisson's ratio
ρ	= Density

ρ_{mn}	= Dimensionless variable defined by (31)
$T_{rr}, T_{\theta\theta}, T_{zz}$	= Normal stresses
$T_{r\theta}$	= Shear stress
$T_{rr}^*, T_{\theta\theta}^*, T_{zz}^*, T_{r\theta}^*$	= Dimensionless variables defined by (31)
Φ	= Temperature difference
Ω_1	= Solution of (11)
Ω_2	= Particular solution of (12)

DISTRIBUTION LIST

<u>No. of Copies</u>	<u>Organization</u>	<u>No. of Copies</u>	<u>Organization</u>
12	Commander Defense Documentation Center ATTN: DDC-TCA Cameron Station Alexandria, VA 22314	2	Commander US Army Mobility Equipment Research & Development Command ATTN: Tech Docu Cen, Bldg. 315 DRSME-RZT Fort Belvoir, VA 22060
1	Commander US Army Materiel Development and Readiness Command ATTN: DRCDMA-ST 5001 Eisenhower Avenue Alexandria, VA 22333	1	Commander US Army Armament Command Rock Island, IL 61202
1	Commander US Army Aviation Systems Command ATTN: DRSAV-E 12th and Spruce Streets St. Louis, MO 63166	1	Commander US Army Harry Diamond Labs ATTN: DRXDO-TI 2800 Powder Mill Road Adelphi, MD 20783
1	Director US Army Air Mobility Research and Development Laboratory Ames Research Center Moffett Field, CA 94035	1	Commander US Army Nuclear Agency ATTN: ACTN-W Fort Bliss, TX 79916
1	Commander US Army Electronic Command ATTN: DRSEL-RD Fort Monmouth, NJ 07703	1	Director US Army TRADOC Systems Analysis Activity ATTN: ATAA-SA White Sands Missile Range NM 88002
1	Commander US Army Missile Command ATTN: DRSMI-R Redstone Arsenal, AL 35809	1	Commander US Naval Surface Weapons Center ATTN: Code WR-42, N. Griff Silver Spring, MD 20910
1	Commander US Army Tank Automotive Development Command ATTN: DRDTA-RWL Warren, MI 48090	1	AFWL/SAT, Mr. A. Sharp Kirtland AFB, NM 87117
			<u>Aberdeen Proving Ground</u> Marine Corps Ln Ofc Dir, USAMSAA